

WISPLC: Search for Dark Matter with LC Circuit

Zhongyue Zhang (张钟月) and Dieter Horns
*Institut für Experimentalphysik, Universität Hamburg,
Luruper Chaussee 149, 22761 Hamburg, Germany*

Oindrila Ghosh
*II. Institut für Theoretische Physik, Universität Hamburg,
Luruper Chaussee 149, 22761 Hamburg, Germany*
(Dated: December 6, 2021)

The focus on dark matter search has expanded to include low-mass particles such as axions or axion-like particles, and novel theoretical schemes extending the phenomenological landscape, within QCD and beyond, also garnered additional interest in recent decades. Assuming dark matter is composed of axions, in presence of a solenoidal magnetic field, they induce a displacement current that gives rise to a toroidal magnetic field. The Weakly Interacting Slender Particle detection with LC circuit (WISPLC) is a precision direct detection experiment that will search for light dark matter candidates such as axion-like particles in parts of the parameter space previously unexplored. We present two detection schemes of the signal in a pickup loop capturing the flux of this toroidal magnetic field. WISPLC operates in a broadband and a resonant scheme where a LC circuit is used to enhance the signal with an expected Q factor $\sim 10^4$. Taking into account the irreducible flux noise of the detector, we estimate the sensitivity of the experiment in the axion mass range between 10^{-11} eV and 10^{-6} eV to reach a detectable axion-photon coupling of $g_{a\gamma\gamma} \approx 10^{-15}$ GeV^{-1} , making it possible to probe mass ranges corresponding to ultralight axions motivated by string theory. The WISPLC experiment is fully funded and currently in the construction phase.

I. INTRODUCTION

Axions are light pseudo-scalar Goldstone bosons that were proposed as a solution to the strong CP problem in quantum chromodynamics (QCD) via the $U(1)_{\text{PQ}}$ Peccei-Quinn (PQ) symmetry breaking [1] [2] [3] and also arise in String theoretical frameworks which, in particular, motivate ultralight species [4]. In recent decades, axions have moved to the forefront of exploring physics beyond the Standard Model, primarily as a potential dark matter candidate.

The mass of axions m_a relates to the PQ scale f_a as:

$$m_a^2 f_a^2 \approx m_\pi^2 f_\pi^2 \quad (1)$$

where m_π and f_π are the mass and decay constant of pions, respectively. Axion-like particles (ALPs) are very similar to QCD axions in terms of their properties but are not constrained by Eq. 1, and therefore, can take a broad range of parameters. Axions interact with photons via the interaction term:

$$\mathcal{L} = \frac{1}{2}(\partial_\mu a)^2 - \frac{1}{2}m_a^2 a^2 - \frac{1}{4}F_{\mu\nu}\tilde{F}^{\mu\nu} + \frac{1}{4}g_{a\gamma\gamma}aF_{\mu\nu}\tilde{F}^{\mu\nu}, \quad (2)$$

where a is the axion field and $F_{\mu\nu}$ and $\tilde{F}_{\mu\nu}$ are respectively the electromagnetic field tensor and its dual. The axion-photon coupling strength $g_{a\gamma\gamma}$ is model-dependent,

$$g_{a\gamma\gamma} = \frac{\alpha}{2\pi f_a} \left[\frac{E}{N} - 1.92(4) \right], \quad (3)$$

where α is the fine structure constant, and E and N are respectively the electromagnetic and colour anomaly coefficients dependent on the choice of axion models such

as DFSZ-I, DFSZ-II, and KSVZ, for which E/N equals to $8/3$, $2/3$, and 0 respectively [5][6] [7] [8] [9]. However, the parameter space window can be further expanded as proposed in [10] [11], and more recently in [12] and [13], which extends the search for QCD axions in the nano-electronVolt (neV) range.

In presence of axions, Maxwell's equation is modified as,

$$\vec{\nabla} \times \vec{B} - \frac{\partial \vec{E}}{\partial t} = g_{a\gamma\gamma} \left(\vec{E} \times \vec{\nabla} a - \vec{B} \frac{\partial a}{\partial t} \right) + \vec{j}_{el}, \quad (4)$$

where \vec{E} and \vec{B} stand for the electric and magnetic field respectively, and \vec{j}_{el} is the electromagnetic current. Equation 4 features the time derivative of the axion field, which is related to the average local axion density as $\langle \rho_a \rangle = \frac{1}{2}\dot{a}^2$.

The characteristic lengthscale of an neV-scale axion is $\sim \mathcal{O}(10^5, \text{m})$, which exceeds the physical dimension of the experiment significantly. Thus, it is safe to assume that axion behaves as a coherent oscillating scalar field in the context of a standard laboratory experiment and we can ignore any spatial variation and assume homogeneity:

$$a(t) = a_0 \cos(m_a t) = \frac{\sqrt{2\rho_{\text{DM}}}}{m_a} \cos(m_a t), \quad (5)$$

where a_0 is the field amplitude, $\rho_{\text{DM}} \approx 0.3 \text{ GeV}/\text{cm}^3$ is the local dark matter density with the assumption $\langle \rho_a \rangle = \rho_{\text{DM}}$. The combination of Eq. 4 and Eq. 5 shows that the external magnetic field induces an axion-sourced current density \vec{j}_a oscillating at the Compton frequency of axions $\nu_a = m_a c^2/h$, where h is Planck's constant and c is the

speed of light. The induced axion current,

$$\vec{j}_a(t) = -g_{a\gamma\gamma} \vec{B} \frac{\partial a}{\partial t}, \quad (6)$$

subsequently generates a perpendicular toroidal magnetic field \vec{B}_a such that $\vec{\nabla} \times \vec{B}_a = \vec{j}_a$. Due to the random dispersion within the dark matter halo following a Maxwell Boltzmann distribution, the axion signal is expected to have a line profile with a bandwidth $\Delta\nu_a$ centered at the Compton frequency $\nu_a = \omega_a/2\pi = m_a c^2/h$ such that $\Delta\nu_a = \nu_a \sigma_v^2$ where the dark matter velocity dispersion $\sigma_v = v/c \sim \mathcal{O}(10^{-3})$ in the Milky Way [14]. The spread of frequencies of axion can be approximated by the inverse of the so-called axion coherence time τ_a , which is limited by its energy spread $\tau_a \sim 1/m_a \sigma_v^2$. For neV axions, we expect $\tau_a \sim 0.66$ s.

The Weakly Interacting Slender Particle detection with LC circuit (WISPLC) experiment proposes to capture \vec{B}_a with a superconducting loop, amplify it with a LC resonant circuit, and measure it with a Superconducting Quantum Interference Device (SQUIDS) magnetometer. The experiment is built upon the concept of detecting the magnetic field generated by the induced axion current in presence of an external magnetic field, as a means of detecting ultralight axions and ALPs in the local galactic halo. Besides the basic broadband detection scheme that uses the entire detector bandwidth, it is also possible to integrate a tunable LC circuit in the readout to enhance the sensitivity in smaller bandwidths. In this work, we present the idea and design of this haloscope experiment with high-field-strength large-scale superconducting magnets.

II. EXPERIMENTAL SETUP FOR WISPLC

The key facility of the WISPLC experiment is a large-scale cryogen-free magnet system with warm bore as shown in Fig. 1. The bore has a diameter of 125 mm and a length of 755 mm. Two concentric solenoids, shown in blue and red, wrapped in superconducting wire, can produce a maximum magnetic field of 14 T at the center of the warm bore. Enclosing the cross-section of magnets, two individually wired superconducting loops shown in green is pre-installed inside the cryostat.

A simple experimental scheme is shown in Fig. 2. The external magnetic field converts axion to an oscillating electric current \vec{j}_a , and creates an oscillating toroidal magnetic field \vec{B}_a perpendicular to \vec{j}_a . According to Faraday's law, \vec{B}_a induces an AC EMF and subsequently an AC current in the pickup loop, which is then amplified by the tunable LC circuit in the readout, and furthermore converted into magnetic field via an input coil. The SQUID magnetometer will measure the AC current through inductive coupling to the input coil. We can express the magnetic flux passing through the pickup loop as

$$\Phi_a(t) = g_{a\gamma\gamma} \sqrt{2\rho_{\text{DM}}} C \sin(m_a t) \quad (7)$$

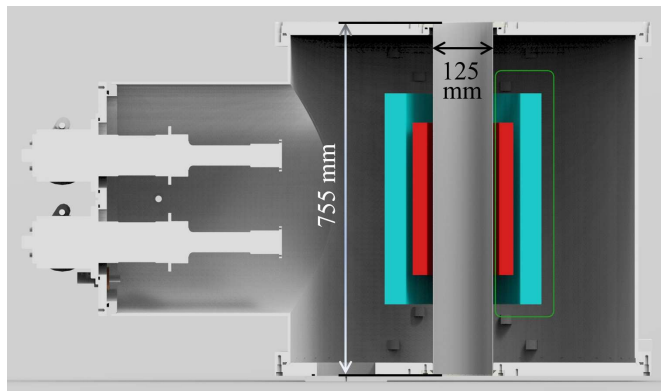


FIG. 1. Model of the large-scale cryogen-free magnet system with a warm bore in the center. The diameter and length of the bore are 125 mm and 755 mm, respectively. Two concentric solenoidal magnets shown in blue and red can produce a maximum magnetic field of 14 T in the center. Shown in green, two individually wired superconducting loops are installed inside the cryostat to enclose the cross-section of the magnets.

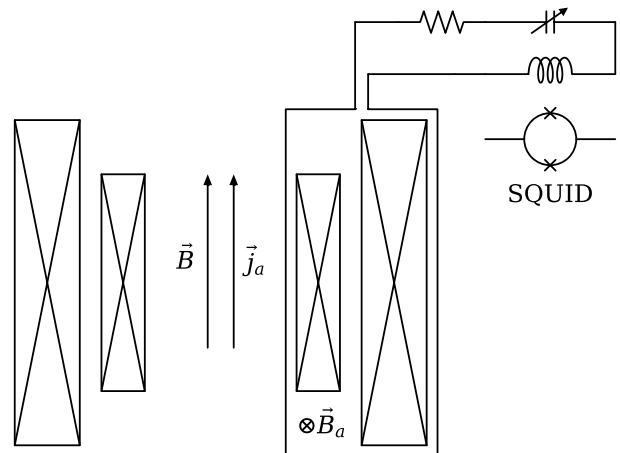


FIG. 2. Schematics of the proposed experimental setup. The four rectangles with crossings represent the windings of two solenoid magnets. The magnets generate a magnetic field \vec{B} which induces an axion-sourced current density \vec{j}_a .

where $C = |\vec{B}_{\text{max}}| V_B$ represents the form factor of the experiment and the effective magnetic volume $V_B = \mathcal{G}_V V_{\text{magnet}}$ can be interpreted as the equivalent volume with a uniform magnetic field \vec{B}_{max} for a given pickup loop geometry. The *specific* form factor \mathcal{G}_V is therefore defined as

$$\mathcal{G}_V = \frac{1}{|\vec{B}_{\text{max}}| V_{\text{magnet}}} \int_{\text{loop}} dS \int_{\text{magnet}} \frac{\vec{B}(\vec{r}) \times (\vec{r} - \vec{r}')}{|\vec{r} - \vec{r}'|^3} \cdot \hat{n} dV, \quad (8)$$

identical to the geometric factor in [15]. For WISPLC, we estimated the relevant values through numerical 2D finite element methods to be $|\vec{B}_{\text{max}}| = 14$ T, $V_{\text{magnet}} = 0.024$ m³, $\mathcal{G}_V = 0.074$. We can readily compare with

values from other experiments as listed in Table I.

TABLE I. Comparison of experimental parameters between WISPLC, ABRA. and SHAFT, $C = |\vec{B}_{\max}|V_{\text{magnet}}\mathcal{G}_V$.

	$ \vec{B}_{\max} $ (T)	\mathcal{G}_V	V_{magnet} (m ³)	C/C_{SHAFT}
SHAFT ^a	1.5	0.108 ^b	9.5×10^{-5}	1
ABRA. ^c	1	0.027	8.9×10^{-4}	1.55
WISPLC	14	0.074	2.4×10^{-2}	1.60×10^3

^a Reference [16].

^b Estimated from the effective volume $\mathcal{G}_V = V_B/V$.

^c Reference [17].

In Table I, we compare our form factor C with those of ABRACADABRA (ABRA.) [15, 17–19] and SHAFT [16] among other experiments that conduct axion search with SQUID magnetometer with various geometries of magnets and pickup loops. By virtue of the large volume and high magnetic field strength of our magnets, the expected C parameter for WISPLC is about three orders of magnitude larger than those for the other experiments listed. We propose two possible readout schemes with SQUID as shown in Fig. 3: A. broadband readout, which utilises direct inductive coupling between the pickup loop and SQUID, in which the bandwidth is only limited by the detector and readout electronics, and B. resonant readout, in which a variable LC resonant circuit is inserted between the pickup loop and SQUID and the superconducting current is enhanced by the quality factor Q of the resonant circuit.

A. Broadband Detection

In the broadband detection scheme, the axion-sourced flux is transferred to the magnetometer through inductive coupling, and the transfer efficiency depends on the properties of the readout circuit, i.e., the mutual inductance M_i of the coupling and the total inductance L_{sys} of the readout circuit:

$$\Phi_{\text{SQUID}}(t) = M_i L_{\text{sys}}^{-1} \Phi_a(t) \quad (9)$$

L_{sys} is the linear addition of the inductances of the pickup loop, coaxial cable, and the coil facing the magnetometer. By virtue of its geometry, the inductance of the pickup loop $\sim 1 \mu\text{H}$ dominates the total inductance of the system and the flux transfer efficiency $\kappa = \Phi_{\text{SQUID}}/\Phi_a$ is estimated to be $\sim 4 \times 10^{-4}$.

The bandwidth of this detection scheme is limited by the SQUID readout electronics. A combination of theoretical estimation and laboratory measurement predicts the bandwidth to be around 3.5 MHz.

B. Resonant Detection

Tunable LC circuit has the advantage of enhancing signal by a large factor Q at the resonant frequency, however, at the expense of introducing additional noise in the system. Similar strategies have been adopted by ADMX SLIC [20] and ABRA. [15, 17, 18]). In the resonant detection scheme, the pickup loop is connected to an LC circuit, and the supercurrent oscillating at the frequency $\omega = 1/\sqrt{LC}$ can be enhanced by its quality factor in a restricted bandwidth $\Delta\omega = \omega/Q$. The magnetic flux coupled to SQUID can be approximated as

$$\Phi_{\text{SQUID}}(t) \approx Q M_i L_{\text{sys}}^{-1} \Phi_a(t) \quad (10)$$

In principle, the quality factor as high as 10^{11} can be achieved, however, one must consider the problem of oversampling at low frequencies when the bandwidth is significantly smaller than the potential intrinsic signal width. As a trade off, [21] picks $Q \sim 4.2(3) \times 10^4$ for the tunable superconducting resonant circuit composed of a toroidal inductor and an electrode, and [22] adopts $Q \sim 10^5$ for a series tunable LC circuit design with four toroidal resonators. For our experiment, we expect a benchmark quality factor of 10^4 .

C. Setup Summary

The setup parameters discussed in this section are summarised in Tab II.

\vec{B}_{\max} (T)	\mathcal{G}_V	V_{magnets} (m ³)	κ	Q
14	0.074	2.4×10^{-2}	4×10^{-4}	10^4

TABLE II. Summary of setup parameters of WISPLC experiment. \vec{B}_{\max} is the maximum magnetic field achievable by the superconducting magnets, \mathcal{G}_V is the specific form factor characterising the geometric contribution of the setup, V_{magnets} is the total volume of the solenoidal magnets; κ is the magnetic flux transfer efficiency between the pickup loop and the SQUIDs, and Q is the quality factor of the resonant circuit.

III. SENSITIVITY ESTIMATE

The typical total flux noise of a SQUID is given by

$$S_{\Phi} = S_{\Phi, \text{SQUID}} + S_{V, \text{amp}}/V_{\Phi}^2 + S_{I, \text{amp}}M_{\text{dyn}}^2 \quad (11)$$

where $S_{V, \text{amp}}$ and $S_{I, \text{amp}}$ are the current and voltage noise from amplifier, and V_{Φ} and M_{dyn} are transfer coefficient and current sensitivity of the front end SQUID, respectively. In terms of noise temperature, we can write

$$S_{\Phi} = 2k_B(\gamma_V T + T_A)R/V_{\Phi}^2 \quad (12)$$

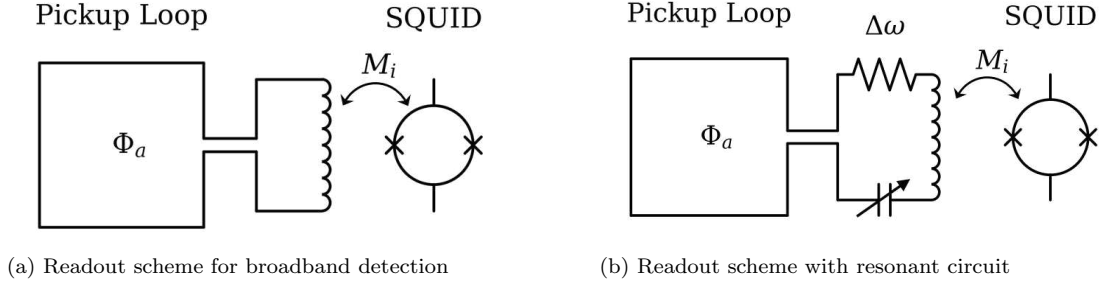


FIG. 3. Two possible readout schemes for axion detection. (a) Readout scheme for broadband detection, the detector is inductively coupled to the pickup loop by an inductor with mutual inductance M_i . (b) Readout scheme with a resonant circuit, the pickup loop is connected to a RLC resonant circuit with bandwidth $\Delta\omega$.

where T is the operating temperature of SQUID, T_A is the effective noise temperature of amplifier (including the parasitic effect of SQUID), R is the shunt resistance of each Josephson junction, and $\gamma_V \approx 8$ [23] or 9 [24] is the reduced white spectral density of the noise voltage V_N across a “bare” SQUID. Our SQUID device is an integrated 2-stage current sensor developed by Magnicon [25] and PTB (Physikalisch-Technische Bundesanstalt) in Berlin, Germany; it consists of an integrated input coil, a single front-end SQUID and a 16 SQUID series array (SSA) as amplifier [26]. The noise measurement of the shielded sensor at 4 K gives the $1/f$ corner frequency ~ 4 Hz and white noise floor in terms of flux quanta Φ_0

$$S_{\Phi}^{1/2} \approx 0.9 \mu\Phi_0/\sqrt{\text{Hz}} \quad (13)$$

which corresponds to an energy resolution of 45 in units of Planck constant, and $\Phi_0 = h/(2e) \approx 2 \times 10^{-15}$ Wb is the magnetic flux quantum. However, it is expected that the input circuit, untuned or tuned, will contribute additional flux noise in terms of noise temperature T_N . In the following section, we discuss the expected noise performances and expected signal-to-noise ratio (SNR) of the two detection schemes.

A. Broadband sensitivity

In the broadband detection scheme, a superconducting pickup loop of inductance L_p connected in series with a pickup coil of inductance L_i is inductively coupled to a SQUID detector, forming a so-called untuned magnetometer, assumed to be operating at T . Using the expression of signal energy for an untuned magnetometer [23], the equivalent noise temperature can be expressed as

$$T_N = T \left[2\gamma_{VJ} \frac{X_i V_{\Phi} M_i^2 \omega}{|Z_T|^2 R} + \gamma_J \frac{V_{\Phi}^2 M_i^4 \omega^2}{|Z_T|^2 R^2} \right] \quad (14)$$

where $X_i = \omega(L_p + L_i)$ is the total input reactance, and $Z_T = \omega^2 M_i^2 / 4R_D + X_i$ is the total input impedance with contribution from SQUID in the limit $\omega L \ll R_D$ while

assuming the dynamic resistance $2R_D \approx R$. $\gamma_J \approx 5.5$ is the reduced spectrum density of the noise current J_N circulating in the SQUID, and $\gamma_{VJ} \approx 6$ is the correlation coefficient between V_N and J_N ; both values are obtained by digital simulation [23]. Combining with parameters of our SQUID detector, we found that T_N can be treated as independent of frequency and $T_N \ll T$. Hence, the noise contribution from the “bare” SQUID and its amplifiers dominates, and we can safely assume $S_{\Phi, \text{untuned}} \approx S_{\Phi}$.

The signal-to-noise ratio (SNR) in the frequency domain generally improves with the observation time t as random noises will be cancelled out via averaging; however, the situation becomes confounding when the observation time exceeds τ_a . The solution is to adapt the Dicke radiometer method in order to treat the axion signal as bandwidth-limited. The SNR can then be summarised as follows:

$$\text{SNR} = \begin{cases} \frac{\Phi_{\text{SQUID}}}{S_{\Phi}^{1/2}} t^{1/2}, & t \leq \tau_a \\ \frac{\Phi_{\text{SQUID}}}{S_{\Phi}^{1/2}} (t\tau_a)^{1/4}, & t > \tau_a \end{cases} \quad (15)$$

For a 2σ detection of neV-scale axions, this leads to an estimated sensitivity for the axion-photon coupling of

$$g_{a\gamma, 2\sigma} \gtrsim 8 \times 10^{-13} \text{ GeV}^{-1} \left(\frac{m_a}{10^{-9} \text{ eV}} \right)^{1/4} \left(\frac{\sigma_v}{10^{-3}} \right)^{1/2} \left(\frac{\rho_{\text{DM}}}{0.3 \text{ GeV/cm}^3} \right)^{-1/2} \left(\frac{\kappa}{4 \times 10^{-4}} \frac{C}{0.025 \text{ m}^3 \text{ T}} \right)^{-1} \left(\frac{t}{100 \text{ days}} \right)^{-1/4} \left(\frac{S_{\Phi}^{1/2}}{0.9 \mu\Phi_0/\sqrt{\text{Hz}}} \right) \quad (16)$$

In Fig. 4, axions with mass and coupling in the blue area would be detectable with WISPLC at 2σ after an integration time of $t_{\text{BB}} = 100$ days. The parameter spaces of two newly proposed frameworks that extend the QCD axion band, photophilic axions [13] and trapped misalignment [12]), are plotted in dark grey lines and light-shaded

grey area, respectively. Due to the limitation of bandwidth of the read-out to 3.5 MHz, the sensitivity deteriorates quickly for axion masses larger than ≈ 10 neV. Given that the sensitivity is not sufficient to cover the expected coupling for some of the theoretical models for axionic dark matter, we consider several ways to improve the sensitivity: (i) longer integration time, (ii) increased form factor, (iii) improved flux transfer efficiency κ , (iv) decreased noise, and (v) resonantly tuned read-out (see next section). The most promising approach is to increase the coupling. This could be achieved by e.g., increasing the geometrical size of the SQUID loop, ultimately exchanging the pickup loop with a SQUID. In Fig. 4, the sensitivity of an improved read-out with a scaled coupling of $\kappa = 2 \times 10^{-3}$ is shown in light-shaded blue. This improved sensitivity is sufficient to constrain the aforementioned dark matter models.

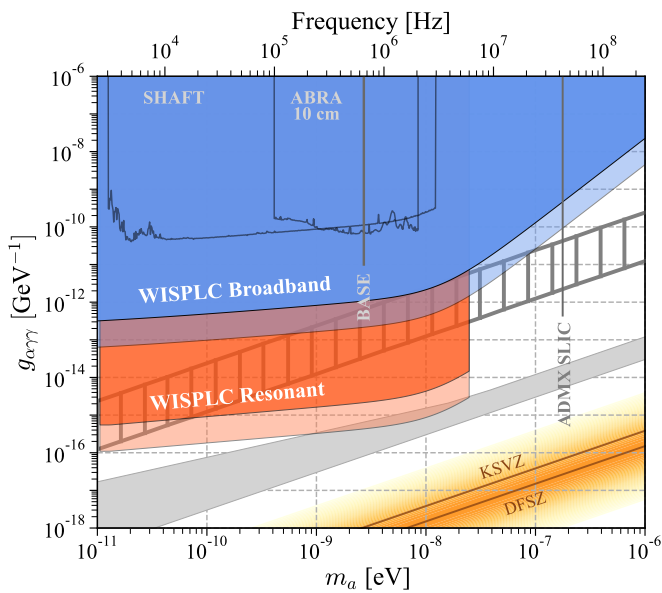


FIG. 4. Anticipated 2σ exclusion limit in the parameter space for both broadband (blue) and resonant (orange) detection schemes. The light-shaded blue and orange areas represent the sensitivity with improved read-out. The total measurement time is 100 days for both schemes. In the resonant scheme, the scan with bandwidth ω/Q (2 min for each frequency with 1 min of effective integration time) will cover the mass range from 10^{-11} eV to 2.5×10^{-8} eV. The favoured parameter space of the trapped misalignment axion model [12] and the photophilic axion model [13] are shown in light-shaded grey area and dark grey lines, respectively.

B. Sensitivity of a tuned circuit

In case of the resonant detection scheme, the search would be limited to a narrow frequency band around the resonant frequency. The bandwidth of the search would be $\Delta\nu \propto 1/Q$, where Q is the quality factor of the circuit. Considering a classical design of a tuned

magnetometer consisting of input capacitance C_i , input inductance $L_p + L_i$ and circuit dissipation R_i , the equivalent noise temperature can be analysed similarly as Eq. 14 with extra thermal noise coming from R_i and $S_{\Phi, R_i}(\nu) = 4k_B T R_i M_i^2 / |Z_T|^2$ [23]. We corroborate that S_{Φ, R_i} significantly exceeds the intrinsic SQUID noise and dominates the input noise contribution. However, with novel LC circuit design consisting of a toroidal superconducting inductor and an electrode in parallel [21], the voltage noise level at resonant frequency of 0.7 MHz is demonstrated to be as low as -90 dBV_{pp}, which is negligible compared to the intrinsic noise level of the SQUID. Further optimisation might be achieved with impedance matching circuit [27]. Here we assume optimal noise performance of the resonant circuit $S_{\Phi, \text{tuned}} \approx S_{\Phi}$.

For the resonant detection, we scan between 10^{-11} eV and 2.5×10^{-8} eV, and assume a 1-min interval for the tuning of the LC circuit which leaves $t_{\text{Res}} \approx 1$ min integration time for each frequency scan. For $m_a \geq 10^{-11}$ eV, the total enhancement on the SNR compared to the broadband detection is

$$Q_{\text{Res}} \approx Q \left(\frac{t_{\text{Res}}}{t_{\text{BB}}} \right)^{1/4} \approx 515 \quad (17)$$

In Figure 4 the orange area shows the 2σ exclusion limit of all resonant bands, and the light-shaded orange area has an improved flux transfer efficiency similar to the light-shaded blue area.

IV. SUMMARY AND OUTLOOK

We have presented an experiment, WISPLC, to search for axions as dark matter in the mass range up to tens of neV. WISPLC is currently under construction. The foreseen sensitivity to the two-photon coupling of axions is improving on existing experimental bounds by two orders of magnitude. The improvement is primarily due to a larger and stronger magnet in comparison to previous experiments. The sensitivity will be reached with a conventional SQUID broadband read-out. A tuned version of the read-out will improve the sensitivity by up to three orders of magnitude in comparison to the broadband readout. This way, we will be sensitive to the detection of axion dark matter with an axion-photon coupling as in recent theoretical proposals [12, 13]. The sensitivity of this setup will not be sufficient to reach the canonical QCD axion range of couplings.

ACKNOWLEDGMENTS

We thank Ciaran O’Hare for useful comments. This project is funded by the Deutsche Forschungsgemeinschaft (DFG, German Research Foundation) under Germany’s Excellence Strategy – EXC 2121 “Quantum Universe” – 390833306 and through the DFG funds for major instrumentation (s/c magnet) DFG INST 152/824-1.

-
- [1] R. D. Peccei and H. R. Quinn, *Physical Review Letters* **38**, 1440 (1977).
- [2] S. Weinberg, *Physical Review Letters* **40**, 223 (1978).
- [3] F. Wilczek, *Physical Review Letters* **40**, 279 (1978).
- [4] A. Arvanitaki, S. Dimopoulos, S. Dubovsky, N. Kaloper, and J. March-Russell, *Physical Review D* **81**, 123530 (2010).
- [5] M. Dine and W. Fischler, *Physics Letters B* **120**, 137 (1983).
- [6] M. Dine, W. Fischler, and M. Srednicki, *Physics Letters B* **104**, 199 (1981).
- [7] A. R. Zhitnitsky, *Soviet Journal of Nuclear Physics* **31**, 260 (1980).
- [8] J. E. Kim, *Physical Review Letters* **43**, 103 (1979).
- [9] M. A. Shifman, A. Vainshtein, and V. I. Zakharov, *Nuclear Physics B* **166**, 493 (1980).
- [10] L. Di Luzio, F. Mescia, and E. Nardi, *Physical Review Letters* **118**, 031801 (2017).
- [11] L. Di Luzio, F. Mescia, and E. Nardi, *Physical Review D* **96**, 075003 (2017).
- [12] L. Di Luzio, B. Gavela, P. Quilez, and A. Ringwald, *arXiv e-prints*, arXiv:2102.01082 (2021), arXiv:2102.01082 [hep-ph].
- [13] A. V. Sokolov and A. Ringwald, *Journal of High Energy Physics* **2021**, 123 (2021).
- [14] L. H. Nguyen, A. Lobanov, and D. Horns, *Journal of Cosmology and Astroparticle Physics* **2019** (10), 014–014.
- [15] Y. Kahn, B. R. Safdi, and J. Thaler, *Phys. Rev. Lett.* **117**, 141801 (2016), arXiv:1602.01086 [hep-ph].
- [16] A. V. Gramolin, D. Aybas, D. Johnson, J. Adam, and A. O. Sushkov, *Nature Physics* **17**, 79 (2021).
- [17] J. L. Ouellet, C. P. Salemi, J. W. Foster, R. Henning, Z. Bogorad, J. M. Conrad, J. A. Formaggio, Y. Kahn, J. Minervini, A. Radovinsky, *et al.*, *Physical Review D* **99**, 052012 (2019).
- [18] J. L. Ouellet, C. P. Salemi, J. W. Foster, R. Henning, Z. Bogorad, J. M. Conrad, J. A. Formaggio, Y. Kahn, J. Minervini, A. Radovinsky, *et al.*, *Physical Review Letters* **122**, 121802 (2019).
- [19] C. P. Salemi, J. W. Foster, J. L. Ouellet, A. Gavin, K. M. W. Pappas, S. Cheng, K. A. Richardson, R. Henning, Y. Kahn, R. Nguyen, N. L. Rodd, B. R. Safdi, and L. Winslow, *Phys. Rev. Lett.* **127**, 081801 (2021).
- [20] N. Crisosto, P. Sikivie, N. S. Sullivan, D. B. Tanner, J. Yang, and G. Rybka, *Phys. Rev. Lett.* **124**, 241101 (2020), arXiv:1911.05772 [astro-ph.CO].
- [21] J. A. Devlin, M. J. Borchert, S. Erlewein, M. Fleck, J. A. Harrington, B. Latacz, J. Warncke, E. Wursten, M. A. Bohman, A. H. Mooser, C. Smorra, M. Wiesinger, C. Will, K. Blaum, Y. Matsuda, C. Ospelkaus, W. Quint, J. Walz, Y. Yamazaki, and S. Ulmer, *Phys. Rev. Lett.* **126**, 041301 (2021).
- [22] H. Nagahama, G. Schneider, A. Mooser, C. Smorra, S. Sellner, J. Harrington, T. Higuchi, M. Borchert, T. Tanaka, M. Besirli, K. Blaum, Y. Matsuda, C. Ospelkaus, W. Quint, J. Walz, Y. Yamazaki, and S. Ulmer, *Review of Scientific Instruments* **87**, 113305 (2016), <https://doi.org/10.1063/1.4967493>.
- [23] J. Clarke, C. D. Tesche, and R. P. Giffard, *Journal of Low Temperature Physics* **37**, 405 (1979).
- [24] D. Drung, in *IEEE/CSC ESAS Supercond. News Forum* (2016).
- [25] "Magnicon", <http://www.magnicon.com/>.
- [26] D. Drung, C. Abmann, J. Beyer, A. Kirste, M. Peters, F. Ruede, and T. Schurig, *IEEE Transactions on Applied Superconductivity* **17**, 699 (2007).
- [27] S. Chaudhuri, K. Irwin, P. W. Graham, and J.ardon, *Optimal impedance matching and quantum limits of electromagnetic axion and hidden-photon dark matter searches* (2021), arXiv:1803.01627 [hep-ph].